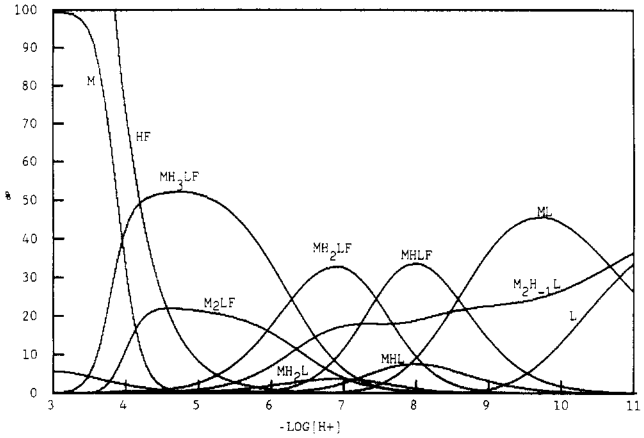

Figure 10. Distribution of species in a solution containing a 1:1 molar ratio of Cu(II) to O-BISTREN in 0.090 M $NaClO_4$ and 0.010 M NaF. $T_{\text{O-BISTREN}} = T_{Cu^{2+}} = 1.000 \times 10^{-3}$ M.

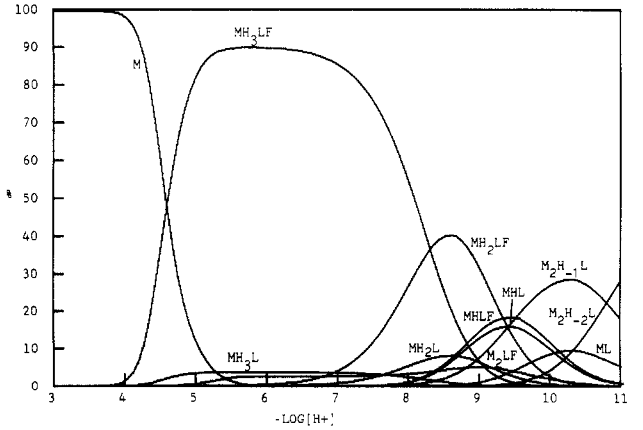

Figure 11. Distribution of species in a solution containing a 1:1 molar ratio of Cu(II) to C-BISTREN in 0.090 M $NaClO_4$ and 0.010 M NaF. $T_{\text{C-BISTREN}} = T_{Cu^{2+}} = 1.000 \times 10^{-3}$ M.

Table V. Fluoride Binding Constants for Copper(II) Complexes of O-BISTREN and C-BISTREN

	log *Q*	
quotient *Q*	O-BISTREN	C-BISTREN
$[M_2LF]/[M_2L][F]$	4.5	3.3
$[MH_3LF]/[MH_3L][F]$	4.1	3.4
$[MH_2LF]/[MH_2L][F]$	3.0	2.7
$[MHLF]/[MHL][F]$	2.7	2.1

[a] μ = 0.100 M (0.090 M $NaClO_4$ + 0.010 M NaF); T = 25.0 °C.

complex dominates solutions made up with 1:1 ligand–metal ion stoichiometry. As seen in Figure 10 the addition of fluoride does not greatly alter that situation, and binuclear complexes dominate the solution from p[H] 4.5–12, even though the ratio of ligand to metal present is 1:1. The main difference in the two systems is that fluoride bridging seems to compete with hydroxide bridging in the low p[H] range, 4.5–6, under which conditions the free hydroxide ion concentration in solution is extremely low. In the case of C-BISTREN (Figure 11), the situation is quite different, and mononuclear complexes, stabilized by fluoride, dominate the system from p[H] 4.5 to 10. The fluoride-bridged triprotonated mononuclear cryptate complex of C-BISTREN seems to be especially stable and is the major species in solution to the exclusion of most others from p[H] 4.5 to 8.5, above which it undergoes successive deprotonation. Finally at p[H] 9.5 the hydroxo-bridged binuclear cryptates become the major species, increasing from 70% of the metal ion at that point to 100% at very high p[H].

Conclusions

This potentiometric study has provided a description of the complex species formed as a function of p[H] by the cryptand ligands O-BISTREN and C-BISTREN in the presence of and in the absence of copper(II) ions and in the presence and in the absence of fluoride ion. The results provide new insights into the nature of hydroxide bridging in the binuclear copper(II)–O-BISTREN cryptate by showing the behavior in the corresponding binuclear copper(II)–C-BISTREN cryptate. The special nature of hydroxide bridging in the binuclear copper(II)–O-BISTREN cryptate and the hydrogen-bonded structure suggested for it in this paper are further supported by the information provided on fluoride ion bridging in these two binuclear cryptate system, whereby it was found that the strength of fluoride ion bridging is very similar for the two binuclear cryptates.

Acknowledgment. This research was supported by a grant, No. A-259, from The Robert A. Welch Foundation.

Registry No. **1**, 64819-97-2; **2**, 99269-13-3; F^-, 16984-48-8; OH^-, 14280-30-9; HF_2^-, 18130-74-0.

Contribution from the Department of Chemistry,
Texas A&M University, College Station, Texas 77843

Synthesis and Characterization of $[Et_4N][M(CO)_5SR]$ and $[Et_4N]_2[M_2(CO)_8(SR)_2]$ Complexes (M = Cr, Mo, W). Ligand Substitution Reactions and X-ray Crystal Structure of $[Et_4N]_2[W_2(CO)_8(SPh)_2]$

Donald J. Darensbourg,* Kathryn M. Sanchez, and Joe Reibenspies

Received March 4, 1988

A series of complexes, $[Et_4N][M(CO)_5SR]$ (M = Cr, Mo, W; R = H, Ph), have been synthesized and characterized by ^1H and ^{13}C NMR and IR spectroscopies. Gentle heating causes these complexes to lose a carbonyl ligand, yielding the doubly bridged sulfur dimers $M_2(CO)_8(\mu\text{-}SR)_2^{2-}$. The X-ray crystal structure of $[Et_4N]_2[W_2(CO)_8(SPh)_2]$ has been determined. The complex crystallizes in the triclinic space group $P\bar{1}$ with unit cell parameters a = 9.8664 (17) Å, b = 9.8566 (22) Å, c = 11.8270 (26) Å, α = 65.790 (16)°, β = 81.710 (16)°, γ = 82.000 (16)°, V = 1034.0 (4) Å^3, and Z = 1. Both mono- and dinuclear metal complexes readily react with phosphorus donor ligands to afford the carbon monoxide substituted complexes *cis*-$M(CO)_4(P)(SR)^-$ (P = PMe_3, $P(OMe)_3$, PPh_3). In addition, the dimers react with 1 atm of carbon monoxide to re-form the mononuclear species $M(CO)_5SR^-$ in quantitative yields. Unsuccessful attempts to insert CO_2, COS, or CS_2 into the M–SR bond in the $M(CO)_5SR^-$ derivatives are noted.

Introduction

The chemistry of metal sulfur complexes has been receiving an increasing amount of attention in recent years. There has been tremendous interest in the synthesis of complexes that model the environment about the transition-metal centers in a number of biologically important enzymes. The structure of the FeMo-co-

Scheme I

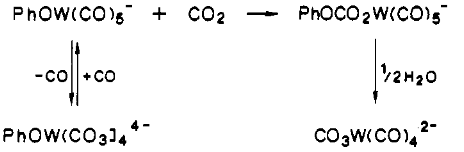

factor of nitrogenase[1] has been a particular focal point of many of these studies. The role of the metal complexes and of various supports in hydrodesulfurization (HDS) catalysis has also been the subject of intense investigations.[2]

We began investigations of group 6 metal carbonyl sulfur complexes as part of our efforts to prepare more stable analogues of certain catalytically active metal alkoxide complexes.[3] Our synthetic efforts in this latter area are summarized in Scheme I for the tungsten phenoxide derivatives. An additional species has been isolated from reactions of $PhOW(CO)_5^-$ in the presence of excess phenoxide and in the absence of CO, which has been shown via X-ray crystallography to be the dimer $(CO)_3W(\mu_2\text{-}OPh)_3W(CO)_3^{3-}$.

Although a number of research groups have used various synthetic procedures to prepare the $M(CO)_5SR^-$ and $M_2(CO)_{10}(\mu\text{-}SR)^-$ complexes (R = H, alkyl, aryl),[4] it has been only recently that the dimers $M_2(CO)_8(SR)_2^{2-}$ (M = Mo,[5] W;[6] R = *t*-Bu, Ph) have been prepared. Herein we report the synthesis of the series of complexes $[Et_4N][M(CO)_5SR]$ and $[Et_4N]_2[M_2(CO)_8(SR)_2]$ (M = Cr, Mo, W; R = H, Ph) typically in yields greater than 90%. These complexes have been fully characterized by infrared and ^{1}H and ^{13}C NMR spectroscopies. The crystal structure of $[Et_4N]_2[W_2(CO)_8(SPh_2)]$ has been determined as well. The lability of the carbonyl ligands has been examined by using phosphine substitution reactions. Solvent studies and reactions with $NaBPh_4$, HOAc, and CO_2 (COS and CS_2) have been used to examine the reactivity of the metal–sulfur bonds.

Experimental Section

Materials and Methods. All reactions were carried out under a dry nitrogen atmosphere on a double-manifold Schlenk vacuum line. Solid transfers were performed under a stream of nitrogen or in an argon-filled drybox. Solvents were dried by distillation from the appropriate reagent and deoxygenated prior to use. Infrared spectra were recorded in 0.10-mm CaF_2 cells on a IBM FT-IR Model 32 spectrometer. ^{1}H and ^{13}C NMR spectra were recorded on a Varian XL-200E spectrometer.

Synthesis of Compounds. [Et$_4$N][SPh]. The procedure used to prepare $[Et_4N][OPh]$[7] was followed. Thiophenol (5.365 g, 0.0487 mol) was placed in a 250-mL three-necked flask containing a stirbar and a reflux condenser. A solution of Et_4NOH in methanol (25% w/w; 40 mL, 0.0536 mol of OH^-) was added via cannula to the flask containing the thiophenol. Dry methanol (50 mL) was added as solvent. This solution was heated to 70 °C for 2 h. After the solution was cooled, the methanol was pumped off in vacuo. Recrystallization from CH_3CN/THF and diethyl ether yielded 10.79 g of $[Et_4N][SPh]$, 92.6% yield of off-white crystals. ^{1}H NMR (CD_3CN, ppm): 1.13 ($(C\mathit{H}_3CH_2)_4N^+$, t); 3.14 ($(CH_3C\mathit{H}_2)_4N^+$, q); 6.49–7.12 ($SC_6\mathit{H}_5^-$, m). ^{13}C NMR (CD_3CN, ppm): 7.75 ($(\mathit{C}H_3CH_2)_4N^+$); 53.0 ($(CH_3\mathit{C}H_2)_4N^+$); 117.7, 127.4, 134.3, 159.6 ($SC_6H_5^-$).

[Et$_4$N][Cr(CO)$_5$SPh]. Et_4NSPh (0.410 g, 1.71 mmol) was placed in a 100-mL Schlenk flask containing a stirbar. $Cr(CO)_6$ (0.374 g, 1.70 mmol) was converted to $Cr(CO)_5{\cdot}THF$ by photolysis in 50 mL of THF. This solution was cannulated to the flask containing the Et_4NSPh. After approximately 10 min of stirring, $Cr(CO)_5{\cdot}THF$ was converted to $Et_4N^+Cr(CO)_5SPh^-$. After the solution was concentrated, diethyl ether (20 mL) was added to precipitate the product. Recrystallization from THF, diethyl ether, and hexane (1:1:1) yielded 0.658 g (89.8%) of $[Et_4N][Cr(CO)_5SPh]$. IR (THF, cm^{-1}) 2043.8 (w), 1915.5 (s), 1869.2 (m). ^{1}H NMR (ppm): cation ($(CD_3)_2CO$), 1.31 ($C\mathit{H}_3$, t), 3.33 ($C\mathit{H}_2$, q); anion ($(CD_3)_2CO$), 122.7, 126.6, 135.5, 150.4 (C_6H_5); carbonyls (THF, $(CD_3)_2CO$), 218.2 (4 CO), 220.7 (1 CO).

[Et$_4$N][Cr(CO)$_5$SH]. Et_4NSH (0.355 g, 2.17 mmol) was placed in a 100-mL Schlenk flask containing a stirbar. $Cr(CO)_6$ (0.461 g, 2.09 mmol) was added to the flask containing the Et_4NSH, followed by the addition of 40 mL of THF. The solution was stirred overnight at room temperature. The flask was fit with a condenser and refluxed for 1 h. The solution was cooled and then filtered. The volume was reduced by half, and diethyl ether and hexane were added to precipitate the product. The compound was recrystallized from THF, ether, and hexane to yield 0.700 g of $[Et_4N][Cr(CO)_5SH]$, 94.0% yield.

Alternatively, the $Cr(CO)_6$ was photolyzed in THF and added to the solid Et_4NSH to prepare $Et_4N^+Cr(CO)_5SH^-$. The complex was precipitated and recrystallized as described above.

[Et$_4$N][Mo(CO)$_5$SPh]. Et_4NSPh (0.772 g, 3.23 mmol) was placed in a 100-mL Schlenk flask containing a stirbar. $Mo(CO)_6$ (0.825 g, 3.13 mmol) was added to the flask under a stream of nitrogen, and THF (50 mL) was added. The solution was stirred, and periodic samples were withdrawn for IR analysis. The reaction was continued until the band due to $Mo(CO)_6$ disappeared. After 48 h, the reaction was complete. The solution was filtered; some solid remained in the flask, which was washed with 2 × 5 mL of THF. These solutions were added to the filtrate. Concentration of the solution followed by addition of 30 mL of hexane yielded a yellow-brown solid. The solid was recrystallized from THF/diethyl ether/hexane to produce 1.40 g of a bright yellow powder (94.2% yield) of $[Et_4N][Mo(CO)_5SPh]$. IR (THF, cm^{-1}): 2056.4 (w), 1921.3 (s), 1865.4 (m). ^{1}H NMR (ppm): cation ($(CD_3)_2CO$), 1.32 ($C\mathit{H}_3$, t), 3.41 ($C\mathit{H}_2$, q); anion ($(CD_3)_2CO$), 6.8–7.4 ($C_6\mathit{H}_5$, m). ^{13}C NMR (ppm): cation ($(CD_3)_2CO$), 7.46 ($\mathit{C}H_3$), $\mathit{C}H_2$ 52.8 ($\mathit{C}H_2$); anion ($(CD_3)_2CO$), 120.0, 127.2, 134.0, 153.5 (C_6H_5); carbonyls (THF, $(CD_3)_2CO$), 207.2 (4 CO), 214.8 (1 CO).

[Et$_4$N][Mo(CO)$_5$SH]. This compound was prepared in a procedure similar to that for the phenyl derivative. Et_4NSH (0.297 g, 1.82 mmol) and $Mo(CO)_6$ (0.458 g, 1.74 mmol) were stirred in 40 mL of THF for 36 h. The solution was filtered and the product precipitated as described above. The crude product was washed with 3 × 10 mL of hexane to remove any $Mo(CO)_6$. Recrystallization from THF and hexane yielded 0.621 g (89.5%) of $[Et_4N][Mo(CO)_5SH]$ as a yellow-brown solid.

[Et$_4$N][W(CO)$_5$SPh]. Et_4NSPh (0.535 g, 2.24 mmol) was placed in a 100-mL Schlenk flask containing a stirbar. $W(CO)_6$ (0.787 g, 2.24 mmol) was converted to $W(CO)_5{\cdot}THF$ by photolysis in 55 mL of THF for 1 h. This solution was cannulated to the flask containing the Et_4NSPh. After 15 min of stirring, $W(CO)_5{\cdot}THF$ was completely converted to $Et_4N^+W(CO)_5SPh^-$. The crude product was precipitated by addition of hexane. Recrystallization from THF/hexane yielded 1.20 g (95.1% yield) of $[Et_4N][W(CO)_5SPh]$. IR (THF, cm^{-1}): 2054.4 (w), 1912.7 (s), 1862.5 (m). ^{1}H NMR (ppm): cation ($(CD_3)_2CO$), 1.36 ($C\mathit{H}_3$, t), 3.45 ($C\mathit{H}_2$, q); anion ($(CD_3)_2CO$), 6.99–7.59 ($C_6\mathit{H}_5$, m). ^{13}C NMR (ppm): cation ($(CD_3)_2CO$), 7.63 ($\mathit{C}H_3$), 53.0 ($\mathit{C}H_2$); anion ((C-

---

(1) (a) Coyl, C. L.; Zumft, W. G. In *Iron-Sulfur Protein Research*; Matsubara, H., Katsube, Y., Wada, K., Eds. Japan Scientific Societies: Tokyo, 1987; pp 185–197. (b) Berg, J. M.; Holm, R. H. In *Metal Ions in Biology*; Spiro, T., Ed.; Wiley: New York, 1982; pp 1–66. (c) Stiefel, E. I.; Cramer, S. P. In Metal Ions in Biology; Spiro, T., Ed.; Wiley: New York, 1982; pp 411–441. (d) Conradson, S. D.; Burgess, B. K.; Newton, W. E.; Hodgson, K. O.; McDonald, J. W.; Rubinson, J. F.; Gheller, S. F.; Mortenson, L. E.; Adams, M. W. W.; Mascharak, P. K.; Armstrong, W. A.; Holm, R. H. *J. Am. Chem. Soc.* **1985**, *107*, 7935. (e) Nelson, M. J.; Levy, M. A.; Orme-Johnson, W. H. *Proc. Natl. Acad. Sci. U.S.A.* **1983**, *80*, 147. (f) Averill, B. A. *Struct. Bonding (Berlin)* **1983**, *53*, 59. (g) Holm, R. H. *Chem. Soc. Rev.* **1981**, *10*, 455.

(2) (a) Weberg, R. T.; Haltiwanger, R. C.; Laurie, J. C. V.; Rakowski DuBois, M. *J. Am. Chem. Soc.* **1986**, *108*, 6242. (b) Zahradnikova, H.; Karnik, Vl.; Beranek, L. *Collect. Czech. Chem. Commun.* **1985**, *50*, 1573. (c) Harris, S.; Chianelli, R. R. *J. Catal.* **1984**, *86*, 400. (d) Valyon, J.; Schneider, R. L.; Hall, W. K. *J. Catal.* **1984**, *85*, 277. (e) Zdrazil, M. *Appl. Catal.* **1982**, *4*, 107. (f) Singhal, G. H.; Espino, R. L.; Sobel, J. E.; Huff, G. A., Jr. *J. Catal.* **1981**, *67*, 457. (g) Singhal, G. H.; Espino, R. L.; Sobel, J. E. *J. Catal.* **1981**, *67*, 446. (h) Kwart, H.; Schuit, G. C. A.; Gates, B. C. *J. Catal.* **1980**, *61*, 128.

(3) (a) Darensbourg, D. J.; Gray, R. L.; Ovalles, C. *J. Mol. Catal.* **1987**, *41*, 329. (b) Darensbourg, D. J.; Gray, R. L.; Ovalles, C.; Pala, M. *J. Mol. Catal.* **1985**, *29*, 285. (c) Tooley, P. A.; Ovalles, C.; Kao, S. C.; Darensbourg, D. J.; Darensbourg, M. Y. *J. Am. Chem. Soc.* **1986**, *108*, 5465. (d) Gaus, P. L.; Kao, S. C.; Youngdahl, K.; Darensbourg, M. Y. *J. Am. Chem. Soc.* **1985**, *107*, 2428. (e) Darensbourg, D. J.; Sanchez, K. M.; Rheingold, A. L. *J. Am. Chem. Soc.* **1987**, *109*, 290.

(4) (a) Darensbourg, D. J.; Rokicki, A.; Kudaroski, R. *Organometallics* **1982**, *1*, 1161. (b) Cooper, M. K.; Duckworth, P. A.; Henrick, K.; McPartlin, M. *J. Chem. Soc., Dalton Trans.* **1981**, 2357. (c) Höfler, M.; Hausmann, H.; Heidelberg, H. A. *J. Organomet. Chem.* **1981**, *213*, C1. (d) Gingerich, R. G. W.; Angelici, R. J. *J. Am. Chem. Soc.* **1979**, *101*, 5604. (e) Schlientz, W. J.; Ruff, J. K. *Inorg. Chem.* **1972**, *11*, 2265. (f) Ruff, J. K.; King, R. B. *Inorg. Chem.* **1969**, *8*, 180.

(5) (a) Zhuang, B.; McDonald, J. W.; Schultz, F. A.; Newton, W. E. *Organometallics* **1984**, *3*, 943. (b) Rosenheim, L. D.; Newton, W. E.; McDonald, J. W. *Inorg. Chem.* **1987**, *26*, 1695.

(6) Zhuang, B.; McDonald, J. W.; Schultz, F. A.; Newton, W. E. *Inorg. Chim. Acta* **1985**, *99*, L29.

(7) McNeese, T. J.; Mueller, T. E.; Wierda, D. A.; Darensbourg, D. J.; Delord, T. J. *Inorg. Chem.* **1985**, *24*, 3465.

$D_3)_2CO)$, 120.6, 127.6, 133.2, 155.6 (C_6H_5); carbonyls (THF, $(CD_3)_2CO$), 200.1 (4 CO), 202.9 (1 CO).

$[Et_4N][W(CO)_5SH]$. This complex was prepared in a manner similar to that described for the phenyl complex. $W(CO)_6$ (0.888 g, 2.52 mmol) was converted to $W(CO)_5 \cdot THF$ by photolysis. The $W(CO)_5 \cdot THF$ solution was added to Et_4NSH (0.418 g, 2.56 mmol) to generate $Et_4N^+W(CO)_5SH^-$. The product was precipitated and recrystallized as described above to yield 1.14 g (92.4%) of $[Et_4N][W(CO)_5SH]$.

$[Et_4N]_2[M_2(CO)_8(SPh)_2]$ (M = Cr, Mo, W). Procedure 1. Approximately equimolar amounts of the metal hexacarbonyl (1–2 g) and Et_4NSPh were weighed out, transferred to a 100-mL Schlenk flask containing a stirbar, and degassed. From the reported procedures for M = Mo[5] and M = W,[6] CH_3CN (50 mL)[8] was added to the solids and the mixture was stirred overnight and then heated to 60 °C for 4–8 h. The solutions were pumped to dryness and washed with THF to remove any unreacted $M(CO)_6$ and $Et_4N^+M(CO)_5SPh^-$. The yellow-brown solids were dissolved in 20 mL of CH_3CN, the solutions were filtered through Celite, and the products precipitated upon the addition of 40 mL of diethyl ether. Yellow crystals were isolated, the tungsten derivative being subjected to an X-ray crystallographic determination. Typical yields were 60–70%. This method was found to be unsuitable for the Cr and SH derivatives.

Procedure 2. The metal sulfur dimers were also prepared by the reaction of the metal hexacarbonyls (M = Cr, Mo, W) and Et_4NSR (R = H, Ph) in THF. To 1–2 g of $M(CO)_6$ and a slight excess (less than 2-fold) of Et_4NSR, in a 100-mL Schlenk flask, was added 50 mL of THF. The solutions were then stirred for 1–2 weeks (M = Mo, W) or refluxed (M = Cr) for 48 h (R = Ph) or 96 h (R = H). Infrared spectra taken of the THF solutions reveal the disappearance of $M(CO)_6$ and formation of $M(CO)_5SR^-$. As the reaction proceeds, the IR bands due to $M(CO)_5SR^-$ decrease. The products gradually form as yellow precipitates (M = Mo, W) or brown oils (M = Cr). The molybdenum and tungsten solutions were filtered; the solids were washed with THF and recrystallized from CH_3CN and Et_2O as in procedure 1. The chromium products were isolated by cannulating the THF off of the oil. The oil became solid after washing with several portions of diethyl ether. The solid was recrystallized from CH_3CN and Et_2O, yielding orange (R = Ph) or red (R = H) crystals. Yields of the molybdenum and tungsten dimers synthesized by this method were generally greater than 90%.

Reactions with Phosphines. Preparation of $[Et_4N][$*cis*$\text{-}M(CO)_4(L)SR]$ (L = PMe_3, $P(OMe)_3$; R = H, Ph; M = Cr, Mo, W). In the drybox, approximately 0.1 g of $[Et_4N][M(CO)_5SR]$ was placed in a 50-mL round-bottom flask containing a stirbar; THF (5–10 mL) was added as solvent. Initial infrared spectra were obtained before the additions of the phosphine. The phosphine, PMe_3 or $P(OMe)_3$, was added via syringe to the solution of $M(CO)_5SR^-$. Stoichiometric equivalents of the phosphine were added as well as 5–20-fold excess. The reactions were monitored by infrared spectroscopy until complete formation of the *cis*-$M(CO)_4(L)SR^-$ product was observed. Once the reaction was complete, the products were rapidly precipitated by the addition of 20 mL of hexane. The solution was removed via cannula, and the products were washed with 4 × 5 mL of diethyl ether. The products were recrystallized from THF and hexane. Yields were typically 60%. However, no attempts were made to maximize the yields.

Preparation of $[Et_4N][M(CO)_4(PPh_3)SR]$ (M = Mo, W). The complexes were prepared by a procedure similar to that described above for the PMe_3 and $P(OMe)_3$ derivatives. The reactions were performed in 25-mL Schlenk tubes. Excess PPh_3 was added (5–10-fold) to the THF solutions under a flow of nitrogen. The products were precipitated and recrystallized as described above. The chromium derivative was not isolated as the reaction did not go to completion in the presence of a 40-fold excess of PPh_3.

Preparation of $[Et_4N][M(CO)_4(\eta^1\text{-dppe})SR]$ (M = Cr, Mo, W). The complexes were prepared as described for the $[Et_4N][M(CO)_4(PPh_3)SR]$ complexes. $[Et_4N][M(CO)_5SR]$ and dppe (dppe = 1,2-bis(diphenylphosphino)ethane) were reacted in 1:1 mole ratios. After complete formation of the $M(CO)_4(\eta^1\text{-dppe})SR^-$ complexes was observed in the infrared spectra, the products were precipitated upon the addition of hexane. Although the $[Et_4N][M(CO)_4(\eta^1\text{-dppe})SR]$ products could be isolated in this manner, all efforts at recrystallization led to formation of the $M(CO)_3(\eta^2\text{-dppe})SR^-$ complexes.

Preparation of $[Et_4N][$*fac*$\text{-}M(CO)_3(PR_3)_2SR]$ (M = Mo, W; PR_3 = PMe_3, $P(OMe)_3$). These complexes were prepared in the same manner as described above for the mono(phosphine) complexes. In these reactions, a 10-fold excess of PMe_3 or a 20-fold excess of $P(OMe)_3$ was added. After initial formation of $M(CO)_4(PR_3)SR^-$, as observed in the infrared spectra, prolonged stirring leads to the formation of the bis(phosphine) complexes *fac*-$M(CO)_3(PR_3)_2SR^-$. The products were isolated in the same manner as described above for the mono(phosphine) complexes.

Preparation of $[Et_4N][$*fac*$\text{-}M(CO)_3(\eta^2\text{-dppe})SR]$ (M = Cr, Mo, W). These complexes are prepared in the same manner as described above for the η^1-dppe complexes. After initial formation of the η^1-dppe complexes was observed in the IR spectra, the reactions were allowed to continue until the bands due to $M(CO)_3(\eta^2\text{-dppe})SR^-$ were the only bands present in the spectra. The products were precipitated with hexane, washed with ether, and recrystallized from acetone/ether/hexane.

Reactions of $[Et_4N]_2[M_2(CO)_8(SR)_2]$. Reaction with Carbon Monoxide (M = Cr, Mo, W; R = H, Ph). The $[Et_4N]_2[M_2(CO)_8(SR)_2]$ complexes (0.2–0.4 g) were dissolved in 30 mL of CH_3CN in 50-mL Schlenk flasks containing stir bars. The flasks were evacuated and refilled with 1 atm of carbon monoxide. The solutions were stirred, and periodic samples were withdrawn for infrared analysis. After 10 min (M = Cr), 30 min (M = Mo), or 2 h (M = W), complete conversion to the $M(CO)_5SR^-$ complexes was observed. The CH_3CN was removed in vacuo, and the products were recrystallized from THF/hexane. Yields of $[Et_4N][M(CO)_5SR]$ prepared in this manner always exceeded 95%.

Infrared Solvent Studies. Infrared spectra of the complexes were recorded in a series of solvents: THF, acetone, acetonitrile, and methanol. Each complex was initially dissolved in THF, and an infrared spectra was recorded. These spectra were used as the standards. The THF was then pumped off, and a second solvent was added. The infrared spectrum of the complex in the second solvent was recorded. The solution was again pumped to dryness, and the solid was redissolved in THF. Again the infrared spectrum of the THF solution was recorded to ensure that no irreversible transformation of the complex occurred.

Reaction of $[Et_4N][M(CO)_5SR]$ with Lewis Acids. HOAc. In a typical experiment, 0.0669 g of $[Et_4N][Mo(CO)_5SPh]$ (0.141 mmol) was placed in a 50-mL round-bottom flask containing a stirbar. THF (5 mL) was added. An infrared spectrum of the starting material was recorded. Excess glacial acetic acid (0.1 mL, 1.7 mmol) was added to the solution via syringe. Infrared spectra were taken periodically to monitor the reaction. The bands due to $M(CO)_5SR^-$ (M = Mo, R = Ph: 2056 w, 1921 s, 1867 s cm^{-1}) are observed to gradually decrease. Bands due to $M_2(CO)_{10}(\mu\text{-SR})^-$ grow in (M = Mo, R = Ph: 2069 vw, 1944 s, 1872 m cm^{-1}).

$NaBPh_4$. In a typical reaction, 0.2 g of $[Et_4N][Cr(CO)_5SH]$ (0.56 mmol) was placed in a 50-mL Schlenk flask containing a stirbar. THF (20 mL) was added as solvent; $NaBPh_4$ was added to the solution under a flow of nitrogen. In separate experiments, 2, 10, 20, or 40 equiv of $NaBPh_4$ was added. The reactions were monitored by periodically withdrawing samples of the solution for IR analysis. Initial shifts in the infrared bands were observed to higher wavenumber, although not greater than 5 cm^{-1}. The infrared bands due to the $M(CO)_5SR^-$ complexes gradually decreased concomitant with the appearance of new sets of bands. These new bands indicate the presence of the complexes $M_2(CO)_{10}(\mu\text{-SR})^-$.

Attempts at Insertion Reactions. $[Et_4N][Cr(CO)_5SPh]$ + CO_2, COS. In a typical experiment 0.21 g of $[Et_4N][Cr(CO)_5SPh]$ was placed in a 50-mL Schlenk flask containing a stirbar. THF (20 mL) was added as solvent. An infrared spectrum of the starting material was recorded. The flask was evacuated and refilled with 1 atm of CO_2 (or COS). The solution was stirred, and periodically samples were withdrawn for IR analysis. After 1 week of stirring the solution, no changes were observed in the IR spectra. Alternatively, the THF solution of $Cr(CO)_5SPh^-$ was transferred to a Fischer–Porter cell. CO_2 (100 psi) was added and the solution stirred. Periodic IR analysis of the solution revealed no reaction was occurring. After 1 week under 100 psi of CO_2 no observable reaction occurred. The solution was pumped to dryness, and the residue was redissolved in THF. Recrystallization of these solutions led to isolation of the starting material in >98% yield.

$[Et_4N][Cr(CO)_5SPh]$ + CS_2. $[Et_4N][Cr(CO)_5SPh]$ (0.195 g, 0.452 mmol) was dissolved in 20 mL of THF in a 50-mL Schlenk flask containing a stirbar. The IR spectrum of the starting solution was recorded (2044 w, 1916 s, 1866 m cm^{-1}). CS_2 (0.27 mL, 4.5 mmol, 10 equiv) was added. After 24 h a new species appeared to be growing in with bands at 1994 w, 1881 m, and 1819 w cm^{-1}. More CS_2 (0.28 mL, 10 equiv) was added. After the mixture was stirred for another 24 h, only a slight increase in the intensity of the bands due to the unknown species was observed. The solution was then refluxed for 45 min. The infrared bands due to the new species almost completely disappeared. A significant amount of precipitate also formed. The solution was filtered and the precipitate dried. Some of the precipitate was soluble in CH_3CN, revealed the presence of $Cr_2(CO)_8(SPh)_2^{2-}$. However, most did not dissolve, remaining a dark brown solid.

$[Et_4N][Mo(CO)_5SPh]$ + CO_2, COS. These experiments were performed in the same manner as those with the chromium complex.

---

(8) Smith, D. A.; Zhuang, B.; Newton, W. E.; McDonald, J. W.; Schultz, F. A. *Inorg. Chem.* **1987**, *26*, 2524.

Table I. Crystallographic Data

mol formula	$C_{36}H_{50}N_2O_8S_2W_2$
fw	1100.6
space group	$P\bar{1}$
a, Å	9.8664 (17)
b, Å	9.8566 (22)
c, Å	11.8270 (26)
α, deg	65.790 (16)
β, deg	81.710 (16)
γ, deg	82.000 (16)
V, Å^3	1034.0 (4)
temp, °C	20 (1)
Z	1
D(calcd), g cm^{-3}	1.77
radiation	Mo Kα (λ = 0.71073 Å)
μ, cm^{-1}	57.89
R	0.0335
R_w	0.0486

$[Et_4N][Mo(CO)_5SPh]$ was dissolved in THF and reacted with 1 atm of CO_2 or COS in a Schlenk flask or 100 psi of CO_2 in a Fischer–Porter cell. After 1 week of stirring the solutions, no new products were observed in the IR spectrum of the THF solutions. However, a significant amount of yellow precipitate formed. After removal of the CO_2 or COS atmosphere, the $Mo(CO)_5SPh^-$ solution was filtered to remove the solid, which was recrystallized. The IR spectrum of the solid material in CH_3CN indicated the formation of $[Et_4N]_2[Mo_2(CO)_8(SPh)_2]$.

$[Et_4N][Mo(CO)_5SPh] + CS_2$. This reaction was performed in the same manner as with the chromium complex. $[Et_4N][Mo(CO)_5SPh]$ (0.316 g, 0.664 mmol) was dissolved in 25 mL of THF. The IR spectrum of the starting material was recorded (2056 w, 1921 s, 1867 cm^{-1}). CS_2 (0.4 mL, 6.6 mmol) was added. After 24 h a new species was observed with IR bands at 2004 w, 1888 ms, and 1826 mw cm^{-1}, a pattern similar to that for the chromium complex. Ten more equivalents of CS_2 was added. The IR bands of the starting material decreased to less than half of their original absorbance height, and the new species appeared to be the major component of the solution. CS_2 (15 equiv) was added in an effort to completely convert the $Mo(CO)_5SPh^-$ to the new species. However, the reaction still did not go to completion. A significant amount of brown-red precipitate formed. The solution was filtered. Some of the solid was $Mo_2(CO)_8(SPh)_2{}^{2-}$. As in the chromium reaction, most of the brownish solid remained insoluble.

$[Et_4N][W(CO)_5SPh] + CO_2$, COS. These reactions were performed in the same manner as those of chromium and molybdenum with 1 atm and 100 psi of CO_2 and 1 atm of COS. After 1 week of reaction, the IR spectra indicated the presence of no new species. A considerable amount of yellow precipitate formed. The precipitate dissolved in CH_3CN and was identified as $[Et_4N]_2[W_2(CO)_8(SPh)_2]$.

$[Et_4N][W(CO)_5SPh] + CS_2$. Procedure 1. $[Et_4N][W(CO)_5SPh]$ (0.143 g, 0.254 mmol) was dissolved in 20 mL of THF. Approximately 10 equiv (0.16 mL) of CS_2 was added to the solution. After 4 days of reaction, no new species were observed in the IR spectra. A significant amount of $[Et_4N]_2[W_2(CO)_8(SPh)_2]$ formed as a yellow precipitate.

Procedure 2. $[Et_4N][W(CO)_5SPh]$ (0.0572 g, 0.102 mmol) was dissolved in 10 mL of THF. CS_2 (~0.06 mL, 10 equiv) was added to the solution. Five milliliters of the solution was placed in a 10-mL stainless-steel microreactor. Argon pressure (500 psi) was added in an effort to increase the possibility of insertion occurring. Samples were withdrawn, and their IR spectra were recorded each day for 4 days. No changes in the infrared spectra were observed. The $[Et_4N][W(CO)_5SPh]$ was recovered quantitatively. No $W_2(CO)_8(SPh_2)^{2-}$ formed as a precipitate under the argon pressure.

X-ray Structure Determination. The X-ray crystallographic experiment was performed on a Nicolet R3m/V diffractometer utilizing graphite-monochromated Mo Kα radiation (λ = 0.71073 Å) at a temperature of 20 ± 1 °C. All crystallographic computations were carried out with the SHELXTL-Plus program library (G. M. Sheldrick, supplied by Nicolet XRD Corp.) on a Microvax II computer. Crystal data and experimental conditions are given in Table I and Table 1S (supplementary material).

A wedge-shaped yellow crystal (0.2 × 0.2 × 0.3 mm) was mounted on a glass fiber with epoxy cement. Preliminary axial photographs were taken. No indication of symmetry was observed in the axial photographs. Likewise, the cell parameters were closely examined by the programs TRACER (SDP crystallographic package, B. A. Frenz and Associates, Inc., College Station, TX 77840) and XCELL (SHELXTL). No indication of higher symmetry was seen. The crystal system was assigned as triclinic. A total number of 3984 reflections were taken. Lorentz and polarization corrections were applied to the data. A semiempirical ellipsoidal absorption correction[9] was performed [$(\mu\tau)_{max}$ = 1.7]: ψ(start) = 0.0, ψ(end) = 345.0, $\Delta(\psi)$ = 15, R(merge)[10] before 0.0779 and after 0.0349. The number of reflections with $|F| > 2.5\sigma(|F|)$ = 3407.

Table II. Atomic Coordinates (×10^4) and Equivalent Isotropic Displacement Parameters (Å^2 × 10^3)[a]

	x	y	z	U(eq)
W	3254 (1)	237 (1)	1065 (1)	39 (1)
S	5675 (2)	−1175 (2)	1235 (2)	42 (1)
C(13)	6637 (7)	−907 (7)	2277 (6)	46 (2)
C(14)	8029 (7)	−740 (8)	2028 (7)	55 (3)
C(15)	8781 (9)	−713 (10)	2921 (8)	63 (3)
C(16)	8174 (9)	−804 (9)	4038 (8)	65 (3)
C(17)	6787 (9)	−926 (10)	4312 (7)	68 (4)
C(18)	6006 (8)	−1039 (9)	3466 (7)	61 (3)
C(1)	3973 (8)	1920 (9)	1288 (9)	62 (4)
O(1)	4322 (9)	2815 (9)	1515 (10)	115 (5)
C(2)	1502 (7)	1409 (9)	681 (1)	54 (3)
O(2)	426 (5)	2095 (7)	463 (6)	78 (3)
C(3)	2529 (9)	−1639 (9)	1139 (8)	61 (3)
O(3)	2068 (10)	−2704 (9)	1353 (8)	110 (5)
C(4)	2569 (7)	−384 (9)	2795 (6)	55 (3)
O(4)	2071 (7)	−712 (10)	3833 (5)	91 (3)
N(1)	2104 (7)	5792 (6)	7097 (7)	62 (3)
C(5)	919 (9)	7004 (9)	6870 (8)	66 (3)
C(6)	3380 (10)	6601 (10)	6523 (9)	79 (4)
C(7)	4711 (11)	5573 (13)	6673 (13)	93 (6)
C(8)	2168 (13)	4883 (11)	8462 (10)	95 (5)
C(9)	1947 (13)	4748 (12)	6500 (15)	104 (7)
C(10)	−494 (10)	6457 (12)	7285 (11)	85 (5)
C(11)	2429 (14)	5707 (19)	9203 (11)	125 (7)
C(12)	1832 (20)	5485 (24)	5112 (19)	155 (15)

[a] Equivalent isotropic U defined as one-third of the trace of the orthogonalized $\mathbf{U}_{ij}$ tensor.

The structure was solved by direct methods in $P\bar{1}$ and $P1$ space groups and subsequent difference Fourier syntheses. Examination of the packing diagram (see the supplementary material) and atomic parameters for molecules in the space group $P1$ indicated an apparent center of symmetry at the centroid defined by the plane of the tungsten and sulfur atoms, between the two Et_4N^+ cations. On the basis of this observation the space group $P\bar{1}$ was chosen. All non-hydrogen atoms were refined with anisotropic thermal parameters. Hydrogen atoms were treated as idealized isotropic contributions, and their isotropic values were fixed at 0.05; C–H distances were set equal to 0.96 Å. The phenyl rings of the anion were constrained to rigid, planar hexagons. Atomic coordinates and equivalent isotropic displacement parameters are listed in Table II.

Results

The synthesis of a series of mononuclear and dinuclear group 6 metal thiolates, $[Et_4N][M(CO)_5SR]$ and $[Et_4N]_2[M_2(CO)_8(SR)_2]$ (R = H, Ph), has been accomplished by displacement of CO or a labile ligand (THF or CH_3CN) from the corresponding metal carbonyls. Infrared and ^1H and ^{13}C NMR spectral data for these derivatives may be found in Tables III–VIII. Transformations of these thiolate complexes in the presence of phosphine or phosphite ligands are summarized in Schemes II–IV. Tables IX and X list the infrared data for these substituted derivatives.

Scheme II

$$M(CO)_5SR^- + P \xrightarrow[\text{THF}]{\text{room temp}} cis\text{-}M(CO)_4(P)SR^-$$

$$M = Cr, Mo, W;\ R = H, Ph;\ P = P(OMe)_3,\ PMe_3, PPh_3$$

Scheme III

$$M(CO)_5SR^- + \text{excess } P \xrightarrow[\text{THF}]{\text{room temp}} fac\text{-}M(CO)_3(P)_2(SR)^-$$

$$M = Mo, W;\ P = PMe_3,\ P(OMe)_3$$

$$M = Cr, Mo, W;\ \tfrac{1}{2}\,P = \text{dppe};\ R = H, Ph$$

---

(9) (a) North, A. C. T.; Phillips, D. C.; Matthews, F. S. *Acta Crystallogr., Sect. A: Cryst. Phys., Diffr., Theor. Gen. Crystallogr.* **1968**, *A24*, 351. (b) Walker, N.; Stuart, D. *Acta Crystallogr., Sect. A: Found. Crystallogr.* **1983**, *A39*, 158.

(10) $R(\text{merge}) = \sum N[(w(F_{mean} - F)^2)]/\sum[(N-1)[\sum(wF^2)]]^{1/2}$.

Scheme IV

$$M_2(CO)_8(SR)_2^{2-} + 2L \xrightarrow[CH_3CN]{\text{room temp}} 2\ cis\text{-}M(CO)_4(L)(SR)^-$$

M = Cr, Mo, W; R = H, Ph; L = CO, PMe_3, $P(OMe)_3$

M = Mo, W; R = H, Ph; L = PPh_3, $P(OPh)_3$

Efforts were directed toward the synthesis of tetranuclear group 6 metal thiolate complexes, $M_4(CO)_{12}(\mu_3\text{-}SR)_4^{4-}$. These complexes would be analogous to the metal(I) sulfur tetramers of manganese and rhenium[11] and would be related to the alkoxide and hydroxide tetramers of chromium, molybdenum, and tungsten.[7,12] The M_4X_4 core (X = O, S) in all of these derivatives exists as a distorted cube in which the metal and X atoms occupy alternate corners. Prolonged refluxing of $[Et_4N][SR]$ with $M(CO)_6$ or $M(CO)_3(CH_3CN)_3$ leads only to formation of the dimers $M_2(CO)_8(SR)_2^{2-}$. Similarly, photolysis of the $M_2(CO)_8(SR)_2^{2-}$ complexes in acetonitrile under a nitrogen purge does not lead to the formation of the tetranuclear compounds.

Solid-State Structure of $[Et_4N]_2[W_2(CO)_8(SPh)_2]$. The structure of the tungsten tetracarbonyl thiophenoxide dimer has been determined by X-ray crystallography. Figures 1 and 2 illustrate various views of the dianion. Pertinent bond distances and bond angles are listed in Tables XI and XII, respectively. The metal centers can be observed in Figure 1 to be in identical octahedral environments, each with four terminal carbonyl ligands and half of each bridging thiophenoxide group. There is an inversion center present. The two tungsten atoms are separated by a nonbonding distance of 4.056 Å. The carbonyl ligands trans to the tungsten–sulfur bonds have tungsten–carbon distances 0.10 Å shorter than the tungsten–carbon bonds of the cis carbonyls. The average tungsten–sulfur distance is 2.59 Å. The phenyl groups are in an anti configuration with one group shown bent down in front of the molecule and the second phenyl group bent up in back of the molecule.

Looking down the tungsten–tungsten axis (Figure 2) offers a better view of the anti arrangement of the thiophenoxide groups. Perhaps it is this configuration that prevents the dimers from forming tetranuclear species as are known for manganese and rhenium thiolate complexes. It has been shown by ^1H NMR data that $[Mn(CO)_4SH]_2$[13] and $[W(CO)_4SR]_2$[14] (R = CH_3, $i\text{-}C_3H_7$, C_2H_5) exist as both syn and anti isomers.

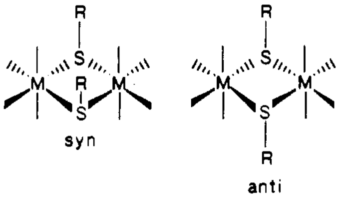

Table III. Infrared Data for $[Et_4N][M(CO)_5SR]$ Complexes (THF, cm^{-1})

M	R	ν_{CO} $A_1^{(2)a}$	E	$A_1^{(1)b}$
Cr	H	2042 w	1912 s	1861 m
Cr	Ph	2044 w	1916 s	1866 m
Mo	H	2057 w	1918 s	1865 m
Mo	Ph	2056 w	1921 s	1865 m
W	H	2053 w	1909 s	1856 m
W	Ph	2054 w	1912 s	1863 m

[a] Symmetric CO stretching motion involving primarily the equatorial CO ligands. [b] Symmetric CO stretching motion involving primarily the axial CO ligand.

Table IV. ^1H NMR Data for $[Et_4N][M(CO)_5SR]$ ($(CD_3)_2CO$, ppm)

M	R	CH_3	CH_2	SH	SC_6H_5
Cr	H	1.35 (t[a])	3.46 (q)	−4.75 (s)	
Cr	Ph	1.31 (t)	3.33 (q)		6.85–7.61 (m)
Mo	H	1.39 (t)	3.49 (q)	−4.01 (s)	
Mo	Ph	1.32 (t)	3.41 (q)		6.48–7.45 (m)
W	H	1.40 (t)	3.50 (q)	−3.51 (s)	
W	Ph	1.35 (t)	3.43 (q)		6.92–7.45 (m)

[a] Abbreviations: s = singlet; t = triplet; q = quartet; m = multiplet.

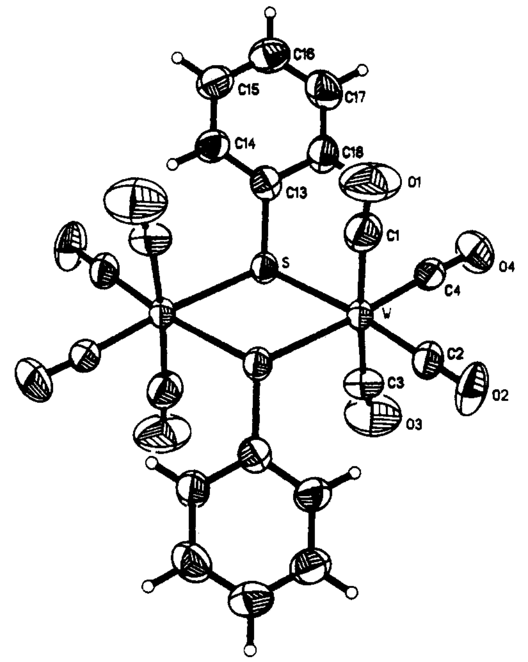

Figure 1. ORTEP view of $W_2(CO)_8(\mu\text{-}SPh)_2^{2-}$. The thermal ellipsoids are drawn at the 50% probability level.

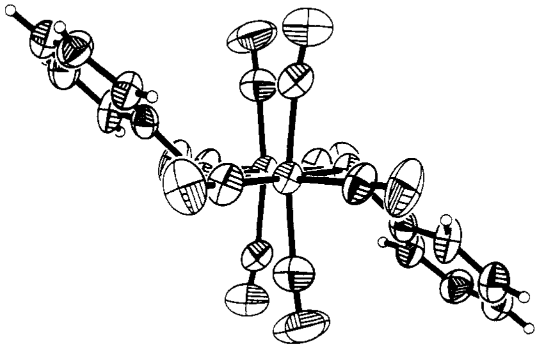

Figure 2. View of $W_2(CO)_8(\mu\text{-}SPh)_2^{2-}$ down the tungsten–tungsten axis.

For the manganese(I) complex, formation of the tetranuclear species may proceed through loss of two carbonyl ligands from the dimers followed by addition of two *syn*-$[Mn(CO)_3SH]_2$ unsaturated species, thus forming the $[Mn(CO)_3SH]_4$ product. There is no evidence in the ^1H or ^{13}C NMR spectra of the zerovalent group 6 derivatives to indicate the presence of the syn isomer. Furthermore, investigation of several different crystals of $[Et_4N]_2[W_2(CO)_8(SPh)_2]$ indicated that they were all isomorphous.[15] The space-filling model of $W_2(CO_8(SPh)_2^{2-}$ (sup-

---

[11] (a) Jaitner, P. *J. Organomet. Chem.* **1981**, *210*, 353. (b) Harrison, W.; Marsh, W. C.; Trotter, J. *J. Chem. Soc., Dalton Trans.* **1972**, 1009. (c) Abel, E. W.; Harrison, W.; McLean, R. A. N.; Marsh, W. C.; Trotter, J. *J. Chem. Soc., Dalton Trans.* **1970**, 1531. (d) Abel, E. W.; Hendra, P. J.; McLean, R. A. N.; Qurashi, M. M. *Inorg. Chim. Acta* **1969**, *3*, 77. (e) Johnson, B. F. G.; Pollock, P. J.; Williams, I. G.; Wojcicki, A. *Inorg. Chem.* **1968**, *7*, 831. (f) Braterman, P. S. *J. Chem. Soc. A* **1968**, 2907. (g) Jenkins, C. R. *J. Organomet. Chem.* **1968**, *15*, 441. (h) Braterman, P. S. *Chem. Commun.* **1968**, 91. (i) Abel, E. W.; Crosse, B. C. *J. Chem. Soc. A* **1966**, 1141. (j) Osborne, A. G.; Stone, F. G. A. *J. Chem. Soc. A* **1966**, 1143.

[12] (a) McNeese, T. J.; Cohen, M. B.; Foxman, B. M. *Organometallics* **1984**, *3*, 552. (b) Albano, V. G.; Bellon, P. L.; Ciani, G.; Manassero, M. *J. Chem. Soc., Dalton Trans.* **1969**, 1242.

[13] Küllmer, V.; Vahrenkamp, H. *Chem. Ber.* **1976**, *109*, 1560.

[14] Winter, A.; Scheidsteger, O.; Huttner, G. *Z. Naturforsch., B: Anorg. Chem., Org. Chem.* **1983**, *38B*, 1525.

Table V. ^{13}C NMR Data for $[Et_4N][M(CO)_5SR]$ ($(CD_3)_2CO$, ppm)

				SC_6H_5[a]				CO[b]	
M	R	CH_3	CH_2	C_a	C_b	C_c	C_d	cis	trans
Cr	H	7.50	52.86					223.0	227.6
Cr[c]	Ph	7.57	52.86	122.7	126.6	135.5	150.4	218.2	220.7
Mo	H	7.67	52.89					208.8	214.9
Mo	Ph	7.46	52.77	120.1	127.2	134.0	153.5	207.2	214.8
W	H	7.39	52.78					201.0	203.9
W	Ph	7.50	52.80	120.6	127.4	134.1	155.6	200.7	202.9

[a] Phenyl carbons are assigned as

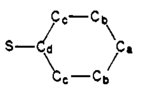

[b] Carbonyl NMR solutions were 3.0-mL THF solutions of $[Et_4N][M(^{13}CO)_5SR]$ with 0.5 mL of $(CD_3)_2CO$ added unless otherwise noted. [c] Solution was 3.0 mL of CH_3CN with 0.5 mL of CD_3CN added; natural-abundance spectrum.

Table VI. Infrared Data for $[Et_4N]_2[M_2(CO)_8(SR)_2]$ (CH_3CN, cm^{-1})

M	R	ν_{CO}			
Cr	H	1996 w	1889 s	1838 m	1808 ms
Cr	Ph	2000 w	1891 s	1839 m	1806 ms
Mo	H	1990 w	1892 s	1841 m	1790 m
Mo	Ph	1995 w	1897 s	1843 m	1798 m
W	H	1985 w	1883 s	1836 m	1789 m
W	Ph	1988 w	1886 s	1839 m	1794 m

Table VII. ^1H NMR Data for $[Et_4N]_2[M_2(CO)_8(SR)_2]$ (CD_3CN, ppm)

M	R	CH_3	CH_2	SH	SC_6H_5
Mo	H	1.20 (t)	3.16 (q)	−2.45 (s)	
Mo	Ph	1.18 (t)	3.17 (q)		6.85–7.77 (m)
W	H	1.20 (t)	3.22 (q)	−1.36 (s)	
W	Ph	1.16 (t)	3.13 (q)		6.85–7.74 (m)

plementary material) clearly illustrates that the sulfur atoms still have open faces that appear to be available for metal bonding. If two metal centers would coordinate to the sulfur atoms, they would not be in the proper orientation to form the cubane tetrameric unit.

The structure of the anionic complex $W_2(CO)_8(SPh)_2^{2-}$ may be compared with the previously reported structures of the neutral W(I) complexes $W_2(CO)_8(S\text{-}t\text{-}Bu)_2$[16] and $W_2(CO)_8(SCH_3)_2$[14] and the anionic Mo(0) derivative $[Et_4N]_2[Mo_2(CO)_8(SCH_2CO_2Et)_2]$.[17,18] Overall, these compounds possess the same geometry. The variations in the distances M–S and M–M and the angles S–M–S′ and M–S–M′ listed in Table XIII are consistent with what might be anticipated for M(0) versus M(I) complexes. The metal–sulfur distances in the W(I) compounds are shorter by approximately 0.1 Å than the metal–sulfur distances in the W(0) and Mo(0) complexes. Stronger interaction of the M^+ centers with the SR^- ligands would lead to shorter metal–sulfur bond lengths. The W(I) compounds both possess tungsten–tungsten single bonds with distances of 2.988 and 2.969 Å for the *tert*-butyl and methyl derivatives, respectively. The W(0) and Mo(0) complexes both possess large metal–metal separations of approximately 4.0 Å, indicating the absence of metal–metal bonding.

Discussion

Lability Studies. The substitution of phosphorus donor ligands for carbon monoxide groups in the $M(CO)_5SR^-$ anions occurs readily at ambient temperature to afford exclusively *cis*-monosubstituted and *fac*-disubstituted derivatives. The rates of these reactions parallel the rates generally observed for CO dissociation in group 6 metal carbonyls; i.e., Mo > Cr > W. The CO-labilizing ability of the SR^- ligands is further evident in that $M(CO)_5SR^-$ derivatives undergo facile CO ligand exchange with ^{13}CO in THF solution at ambient temperature. The ^{13}C NMR spectrum of such a ^{13}C-enriched sample after phosphite substitution, *cis*-$W(CO)_4[P(OMe)_3]SPh^-$, is depicted in Figure 3, clearly illustrating the three different types of CO ligands present in these species.

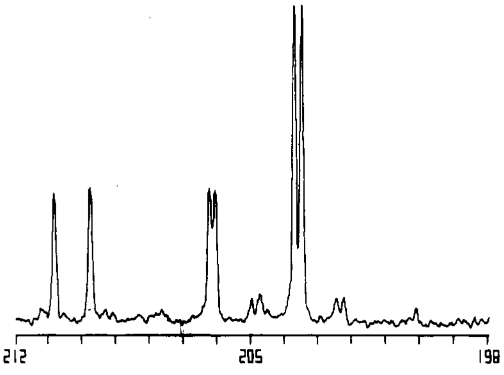

Figure 3. ^{13}C NMR spectrum of $[Et_4N][cis\text{-}W(^{13}CO)_4\{P(OMe)_3\}SPh]$ in $THF/CDCl_3$. The resonance for the two CO ligands cis to both $P(OMe)_3$ and –SPh is at 203.6 ppm (J_{C-P} = 11.1 Hz), whereas the peaks for the CO groups trans to the –SPh and $P(OMe)_3$ ligands are at 206.1 ppm (J_{C-P} = 8.7 Hz) and 210.2 ppm (J_{C-P} = 54.0 Hz), respectively. Only the signal due to the CO groups cis to both $P(OMe)_3$ and –SPh clearly shows ^{185}W satellites, with J_{W-C} = 126.6 Hz.

The metal sulfur dimers are readily cleaved by addition of phosphines without observing $M_2(CO)_{8-n}(P)_n(SR)_2^{2-}$ intermediates, as well as by atmospheric pressures of carbon monoxide (Scheme IV). Similar processes have been observed for the manganese and rhenium thiolate complexes (R = H, CH_3; eq 1).[19]

$$M(CO)_5SR \underset{+CO}{\overset{-CO}{\rightleftharpoons}} [M(CO)_4SR]_2 \underset{+CO}{\overset{-CO}{\rightleftharpoons}} [M(CO)_3SR]_4 \qquad (1)$$

The bis(phosphine) complexes may also be formed if excess phosphine or dppe are employed. In these reactions, the cis metal tetracarbonyl phosphine (or η^1-dppe) thiolate complexes are observed as intermediates. The selectivity of formation of the facial isomers of the $M(CO)_3(PR_3)_2(SR)^-$ complexes is in contrast to related chemistry performed with the neutral $M_2(CO)_8(SR)_2$ complexes (M = Mn, Re; R = H, CH_3, $Sn(CH_3)_3$).[20] Reaction of PMe_3 with $M_2(CO)_8(SR)_2$ forms $M_2(CO)_6(PMe_3)_2(SR)_2$, with one phosphine group on each metal center, and $M(CO)_3(PR)_2SR$, which exists as both facial and meridional-trans isomers.

Reactions of the Bound SR^- Ligand with Acids. The basicities of the SR^- ligands have been examined by measuring the solvent effects on the ν(CO) vibrational modes, as well as by noting the reactivity of the SR^- functionality with the alkali-metal ion Na^+ and with acetic acid.

---

(15) Payne, N. C.; Okura, N.; Otsuka, S. *J. Am. Chem. Soc.* **1983**, *105*, 245.
(16) (a) Hohmann, M.; Krauth-Siegel, L.; Weidenhammer, K.; Schulze, W.; Ziegler, M. L. *Z. Anorg. Allg. Chem.* **1981**, *481*, 95. (b) Schulze, W.; Ziegler, M. L. *Z. Anorg. Allg. Chem.* **1981**, *481*, 78.
(17) Zhuang, B.; Huang, L.; Yang, Y.; Lu, J. *Inorg. Chim. Acta* **1986**, *116*, L41.
(18) Zhuang, B.; Huang, L.; Yang, Y.; Lu, J. *Jiegou Huaxue* **1985**, *4*, 103.
(19) Küllmer, V.; Vahrenkamp, H. *Chem. Ber.* **1976**, *109*, 1569.
(20) (a) Küllmer, V.; Vahrenkamp, H. *Chem. Ber.* **1977**, *110*, 3799. (b) Küllmer, V.; Vahrenkamp, H. *Chem. Ber.* **1977**, *110*, 3810.

Table VIII. ^{13}C NMR Data for $[Et_4N]_2[M_2(CO)_8(SR)_2]$ (CD_3CN, ppm)

				SC_6H_5[a]				CO[b]	
M	R	CH_3	CH_2	C_a	C_b	C_c	C_d	cis	trans
Mo	H	7.28	52.57					213.7	221.9
Mo	Ph	7.22	52.60	121.9	127.1	133.1	151.8	212.4	222.8
W	H	7.83	53.28					209.7	216.9
W	Ph	7.63	52.99	122.3	127.6	133.2	148.6	209.6	216.5

[a] See footnote *a* of Table V for labels a–d. [b] In CH_3CN/CD_3CN.

Table IX. Bond Lengths (Å)

W–S	2.582 (2)	W–S′	2.599 (2)
W–C(1)	2.018 (8)	W–C(2)	1.941 (7)
W–C(3)	2.040 (8)	W–C(4)	1.925 (7)
S–C(13)	1.779 (7)	C(13)–C(14)	1.381 (10)
C(13)–C(18)	1.415 (10)	C(14)–C(15)	1.387 (11)
C(15)–C(16)	1.342 (12)	C(16)–C(17)	1.371 (12)
C(17)–C(18)	1.395 (11)	C(1)–O(1)	1.129 (10)
C(2)–O(2)	1.177 (9)	C(3)–O(3)	1.121 (10)
C(4)–O(4)	1.182 (9)	N(1)–C(5)	1.518 (10)
N(1)–C(6)	1.507 (10)	N(1)–C(8)	1.497 (12)
N(1)–C(9)	1.502 (13)	C(5)–C(10)	1.508 (13)
C(6)–C(7)	1.528 (15)	C(8)–C(11)	1.484 (21)
C(9)–C(12)	1.512 (22)		

Table X. Bond Angles (deg)

W–S–W	103.1	S–W–S′	76.9
C(1)–W–S	90.5 (2)	C(2)–W–S	171.8 (2)
C(2)–W–C(1)	90.2 (3)	C(3)–W–S	87.7 (2)
C(3)–W–C(1)	170.9 (3)	C(3)–W–C(2)	92.9 (3)
C(4)–W–S	101.1 (2)	C(4)–W–C(1)	85.0 (3)
C(4)–W–C(2)	87.1 (3)	C(4)–W–C(3)	86.5 (3)
C(13)–S–W	113.4 (2)	C(14)–C(13)–S	122.3 (5)
C(18)–C(13)–S	119.4 (5)	C(18)–C(13)–C(14)	117.9 (6)
C(15)–C(14)–C(13)	120.8 (7)	C(16)–C(15)–C(14)	121.2 (8)
C(17)–C(16)–C(15)	120.0 (8)	C(18)–C(17)–C(16)	120.7 (8)
C(17)–C(18)–C(13)	119.4 (7)	O(1)–C(1)–W	174.1 (9)
O(2)–C(2)–W	178.7 (7)	O(3)–C(3)–W	170.0 (8)
O(4)–C(4)–W	175.8 (7)	C(6)–N(1)–C(5)	105.5 (6)
C(8)–N(1)–C(5)	110.8 (7)	C(8)–N(1)–C(6)	111.2 (8)
C(9)–N(1)–C(5)	111.2 (8)	C(9)–N(1)–C(6)	110.5 (8)
C(9)–N(1)–C(8)	107.6 (8)	C(10)–C(5)–N(1)	115.4 (7)
C(7)–C(6)–N(1)	114.0 (7)	C(11)–C(8)–N(1)	115.6 (9)
C(12)–C(9)–N(1)	115.0 (10)		

Table XI. Comparative Structural Data for M(0) and M(I) Sulfur Dimers

	$W_2(CO)_8(SPh)_2^{2-}$	$W_2(CO)_8(S\text{-}t\text{-}Bu)_2$
M–S, Å	2.590	2.477
M···M, Å	4.056	2.988
S–M–S′, deg	76.9	105.8
M–S–M′, deg	103.1	74.2

	$W_2(CO)_8(SMe)_2$	$Mo_2(CO)_8(SCH_2CO_2Et)_2^{2-}$
M–S, Å	2.473	2.586
M···M, Å	2.969	3.939
S–M–S′, deg	106.2	80.80
M–S–M′, deg	73.8	99.20

Table XII. Infrared Data for $[Et_4N][\textit{cis}\text{-}M(CO)_4(L)SR]$ (THF, cm^{-1})

M	R	L	ν(CO)			
Cr	H	$P(OMe)_3$	1995 w	1890 sh	1878 s	1825 m
Cr	H	PMe_3	1982 w	1870 s	1860 sh	1810 m
Cr	H	dppe	1988 w	1884 s	1856 sh	1803 m
Cr	Ph	$P(OMe)_3$	1997 w	1873 s		1834 m
Cr	Ph	PMe_3	1985 w	1875 s	1863 sh	1818 m
Cr	Ph	dppe	1990 w	1885 s	1869 sh	1821 m
Mo	H	$P(OMe)_3$	2007 w	1890 s		1826 m
Mo	H	PMe_3	1996 w	1879 s	1862 sh	1813 m
Mo	H	dppe	2003 w	1891 s	1879 sh	1808 m
Mo	H	PPh_3	2000 w	1887 s	1870 sh	1821 m
Mo	Ph	$P(OMe)_3$	2008 w	1895 s		1836 m
Mo	Ph	PMe_3	1999 w	1884 s	1867 sh	1821 m
Mo	Ph	dppe	2003 w	1894 s	1872 sh	1820 m
Mo	Ph	PPh_3	2002 w	1891 s	1870 sh	1827 m
W	H	$P(OMe)_3$	2002 w	1875 s		1821 m
W	H	PMe_3	1994 w	1870 s	1858 sh	1809 m
W	H	dppe	1996 w	1878 s	1860 sh	1810 m
W	H	PPh_3	1993 w	1874 s	1860 sh	1811 m
W	H	$P(OMe)_3$	2003 w	1879 s		1830 m
W	Ph	PMe_3	1992 w	1872 s	1859 sh	1815 m
W	Ph	dppe	1999 w	1883 s		1803 m
W	Ph	PPh_3	2000 w	1879 s	1865 sh	1821 m

Table XIII. Infrared Data for $[Et_4N][\textit{fac}\text{-}M(CO)_3(L)_2SR]$ (THF, cm^{-1})

M	R	2 L	ν(CO)		
Cr	H	dppe	1895 s	1798 ms	1763 ms
Cr	Ph	dppe	1898 s	1803 ms	1787 ms
Mo	H	2 $P(OMe)_3$	1930 s	1844 ms	1794 ms
Mo	H	2 PMe_3	1899 s	1793 ms	1773 ms
Mo	H	dppe	1905 s	1807 ms	1768 ms
Mo	Ph	2 $P(OMe)_3$	1895 s	1837 ms	1804 ms
Mo	Ph	2 PMe_3	1902 s	1793 ms	1781 ms
Mo	Ph	dppe	1908 s	1813 ms	1790 ms
W	H	2 PMe_3	1894 s	1785 s	
W	H	dppe	1897 s	1800 ms	1773 ms
W	Ph	2 $P(OMe)_3$	1887 s	1828 ms	1787 ms
W	Ph	2 PMe_3	1891 s	1784 ms	1755 ms
W	Ph	dppe	1899 s	1802 ms	1769 ms

Solvent Studies. Infrared spectra of the complexes $[Et_4N][M(CO)_5SR]$ were taken in a series of solvents (THF, acetone, acetonitrile, and methanol). The spectroscopic data are listed in Table XIV. Only minor changes in the ν(CO) stretching frequencies in $M(CO)_5SR^-$ complexes were observed as the solvent was changed from THF to acetone or acetonitrile. The most acidic solvent, methanol, created the largest shifts in the CO stretching frequencies to higher wavenumbers. Interaction of methanol with these complexes is proposed to be occurring via a "hydrogen bonding" type adduct as is illustrated by structure A.[21] Protons from the solvent can interact with the lone pairs of electrons on the sulfur atoms. The more acidic the solvent, the stronger the interaction.

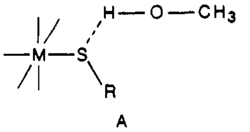

A

This hydrogen-bonding interaction is completely reversible; that is, after the methanol is pumped off and the complex is redissolved in THF, the original THF spectrum is observed. A similar effect was observed in the infrared spectra of the metal formate complex $W(CO)_5OCHO^-$ in THF and methanol.[22]

Addition of $NaBPh_4$. The addition of a 10–40-fold excess of $NaBPh_4$ to solutions of the $M(CO)_5SR^-$ complexes initially leads to the formation of ion-paired $Na^+\cdots S$ adducts similar in structure to the hydrogen-bonding species observed in methanol. Shifts in the CO stretching frequencies to higher wavenumbers are not as significant as those observed upon dissolving the complexes in methanol. In contrast to the solvent interactions, which are re-

---

[21] (a) Ash, C. E.; Delord, T. J.; Simmons, D.; Darensbourg, M. Y. *Organometallics* **1986**, *5*, 17. (b) Darensbourg, M. Y. *Prog. Inorg. Chem.* **1985**, *33*, 221 and references therein.

[22] Darensbourg, D. J.; Ovalles, C. *J. Am. Chem. Soc.* **1984**, *106*, 3750.

Table XIV. Infrared Data for $[Et_4N][M(CO)_5(SR)]$ (cm^{-1})

M	R	solvent	bands			
Cr	H	THF	2042 w	1953 w	1912 s	1861 m
Cr	H	acetone	2043 w		1915 s	1854 m
Cr	H	CH_3CN	2046 w		1917 s	1855 m
Cr	H	CH_3OH	2053 w		1924 s	1873 m
Cr	Ph	THF	2044 w	1959 w	1915 s	1867 m
Cr	Ph	acetone	2044 w		1918 s	1864 m
Cr	Ph	CH_3CN	2047 w		1918 s	1861 m
Cr	Ph	CH_3OH	2053 w		1925 s	1877 m
Mo	H	THF	2054 w		1917 s	1859 m
Mo	H	acetone	2055 w		1920 s	1854 m
Mo	H	CH_3CN	2059 w		1920 s	1861 m
Mo	H	CH_3OH	2063 w		1931 s	1876 m
Mo	Ph	THF	2056 w	1968 w	1921 s	1866 m
Mo	Ph	acetone	2057 w		1923 s	1859 m
Mo	Ph	CH_3CN	2060 w		1924 s	1856 m
Mo	Ph	CH_3OH	2062 w		1932 s	1877 m
W	H	THF	2053 w	1953 w	1909 s	1856 m
W	H	acetone	2057 w		1923 s	1859 m
W	H	CH_3CN	2060 w		1916 s	1857 m
W	H	CH_3OH	2061 w		1920 s	1869 m
W	Ph	THF	2054 w	1958 w	1912 s	1863 m
W	Ph	acetone	2055 w		1914 s	1856 m
W	Ph	CH_3CN	2058 w		1916 s	1855 m
W	Ph	CH_3OH	2060 w		1923 s	1872 m

Table XV. Infrared Data for $[Et_4N][M_2(CO)_{10}(\mu\text{-SR})]$ (THF, cm^{-1})

M	R	ν(CO)		
Cr	H	2062 vw	1937 s	1875 m
Cr	Ph	2061 vw	1939 s	1870 m
Mo	H	2070 vw	1943 s	1875 m
Mo	Ph	2069 vw	1945 s	1870 m
W	H	2070 vw	1935 s	1872 m
W	Ph	2068 vw	1936 s	1868 m

versible, within 30 min of $NaBPh_4$ addition the metal dimers $M_2(CO)_{10}(\mu\text{-SR})^-$ are observed in the infrared spectra (eq 2).

$$2M(CO)_5SR^- + Na^+ \rightarrow NaSR + M_2(CO)_{10}(\mu\text{-SR})^- \quad (2)$$

The interaction of the sodium ion with the lone pairs of electrons on the sulfur ligand must significantly reduce the strength of the metal–sulfur bond. This interaction is sufficient to cleave the transition-metal–sulfur bond. The $M(CO)_5$ fragment then reacts with a $M(CO)_5SR^-$ complex, forming the well-known dimers $M_2(CO)_{10}(\mu\text{-SR})^-$ (see Table XV for ν(CO) infrared data). The rate of formation of the dimers is dependent on the metal, with Cr > Mo ≫ W. The interaction of sodium ions with the sulfur atom of a metal thiolate complex has been observed in the solid-state crystal structure of $[Na(18\text{-crown-}6)][W(CO)_5SH]$.[4b]

The disruption of metal–ligand bonds in $M(CO)_4(L)X^-$ complexes upon addition of alkali-metal salts has been observed in other systems. The abstraction of Cl^- by Na^+ in *cis*-$W(CO)_4(L)Cl^-$ in THF (L = CO, $P(OMe)_3$) is observed spectroscopically, forming *cis*-$W(CO)_4(L)$–THF.[23] Studies on the effect of alkali-metal ions on the insertion reactions of CO_2 into the tungsten–carbon bond of $CH_3W(CO)_5^-$ also reveal similar results.[24] A significant acceleration of the rate of CO_2 insertion for the tungsten methyl complex was observed in the presence of alkali-metal ions. However, subsequent to the insertion process, the alkali-metal ion caused the displacement of the carboxylate ligand from the metal center.

Addition of Acetic Acid. The complexes $M(CO)_5SR^-$ were reacted with 10 equiv of acetic acid in THF (eq 3). The rate

$$2M(CO)_5SR^- + H^+ \rightarrow M_2(CO)_{10}(\mu\text{-SR})^- + RSH \quad (3)$$

of conversion to the singly bridged dimers decreases in the order Cr > Mo > W. Similar results were observed by Angelici and Gingerich[4d] upon the reaction of CF_3SO_3H with $W(CO)_5SH^-$.

Insertion Reactions. The facility with which carbon dioxide, carbonyl sulfide, and carbon disulfide insert into the metal–oxygen bonds of $M(CO)_5OPh^-$ (M = Cr, W)[3e,25] led us to investigate whether similar processes would be observed for the $M(CO)_5SPh^-$ complexes. We anticipated on the basis of the stronger M–S vs M–O bond that if insertion were to occur, longer reaction periods as well as more rigorous conditions would be necessary. Spectroscopic data do not lead us to conclude that these insertion reactions occur (eq 4).

$$M(CO)_5SPh^- + CO_2 \text{ or COS or } CS_2 \rightarrow \text{no insertion products} \quad (4)$$

Acknowledgment. The financial support of this research by the National Science Foundation (Grant CHE 86-03681) and the Robert A. Welch Foundation is greatly appreciated. The X-ray diffraction equipment was funded by a grant from the National Science Foundation.

Registry No. $[Et_4N][SPh]$, 3193-72-4; Et_4NOH, 77-98-5; $[Et_4N][Cr(CO)_5SPh]$, 116148-10-8; $Cr(CO)_6$, 13007-92-6; $Cr(CO)_5{\cdot}THF$, 15038-41-2; $[Et_4N][Cr(CO)_5SH]$, 116148-11-9; $[Et_4N][Mo(CO)_5SPh]$, 116148-75-5; $Mo(CO)_6$, 13939-06-5; $[Et_4N][Mo(CO)_5SH]$, 116148-12-0; $[Et_4N][W(CO)_5SPh]$, 116148-13-1; $W(CO)_6$, 14040-11-0; $W(CO)_5{\cdot}THF$, 36477-75-5; $[Et_4N][W(CO)_5SH]$, 65198-81-4; $[Et_4N]_2[Cr_2(CO)_8(SPh)_2]$, 116148-15-3; $[Et_4N]_2[Mo_2(CO)_8(SPh)_2]$, 90029-16-6; $[Et_4N]_2[W_2(CO)_8(SPh)_2]$, 97092-71-2; $[Et_4N]_2[Cr_2(CO)_8(SH)_2]$, 116184-34-0; $[Et_4N]_2[Mo_2(CO)_8(SH)_2]$, 97092-78-9; $[Et_4N]_2[W_2(CO)_8(SH)_2]$, 97092-77-8; HOAc, 64-19-7; $[Cr_2(CO)_{10}(\mu\text{-SH})]^-$, 45270-67-5; $[Mo_2(CO)_{10}(\mu\text{-SH})]^-$, 81063-76-5; $[W_2(CO)_{10}(\mu\text{-SH})]^-$, 71688-50-1; $[Cr_2(CO)_{10}(\mu\text{-SPh})]^-$, 47598-50-5; $[Mo_2(CO)_{10}(\mu\text{-SPh})]^-$, 116148-74-4; $[W_2(CO)_{10}(\mu\text{-SPh})]^-$, 47598-51-6; $NaBPh_4$, 143-66-8; CO_2, 124-38-9; COS, 463-58-1; CS_2, 75-15-0; $[Et_4N][$*cis*-$Cr(CO)_4[P(OMe)_3]SH]$, 116148-17-5; $[Et_4N][$*cis*-$Cr(CO)_4(PMe_3)SH]$, 116148-19-7; $[Et_4N][$*cis*-$Cr(CO)_4(dppe)SH]$, 116148-21-1; $[Et_4N][$*cis*-$Cr(CO)_4[P(OMe)_3]SPh]$, 116148-23-3; $[Et_4N][$*cis*-$Cr(CO)_4(PMe_3)SPh]$, 116148-25-5; $[Et_4N][$*cis*-$Cr(CO)_4(dppe)SPh]$, 116148-27-7; $[Et_4N][$*cis*-$Mo(CO)_4[P(OMe)_3]SH]$, 116148-29-9; $[Et_4N][$*cis*-$Mo(CO)_4(PMe_3)SH]$, 116148-31-3; $[Et_4N][$*cis*-$Mo(CO)_4(dppe)SH]$, 116148-33-5; $[Et_4N][$*cis*-$Mo(CO)_4(PPh_3)SH]$, 116148-35-7; $[Et_4N][$*cis*-$Mo(CO)_4[P(OMe)_3]SPh]$, 116148-37-9; $[Et_4N][$*cis*-$Mo(CO)_4(PMe_3)SPh]$, 116148-39-1; $[Et_4N][$*cis*-$Mo(CO)_4(dppe)SPh]$, 116148-41-5; $[Et_4N][$*cis*-$Mo(CO)_4(PPh_3)SPh]$, 116184-36-2; $[Et_4N][$*cis*-$W(CO)_4[P(OMe)_3]SH]$, 116148-43-7; $[Et_4N][$*cis*-$W(CO)_4(PMe_3)SH]$, 116148-45-9; $[Et_4N][$*cis*-$W(CO)_4(dppe)SH]$, 116148-47-1; $[Et_4N][$*cis*-$W(CO)_4(PPh_3)SH]$, 116148-49-3; $[Et_4N][$*cis*-$W(CO)_4(PMe_3)SPh]$, 116148-51-7; $[Et_4N][$*cis*-$W(CO)_4(dppe)SPh]$, 116148-53-9; $[Et_4N][$*cis*-$W(CO)_4(PPh_3)SPh]$, 116148-55-1; $[Et_4N][$*fac*-$Cr(CO)_3(dppe)SH]$, 116148-57-3; $[Et_4N][$*fac*-$Cr(CO)_3(dppe)SPh]$, 116148-59-5; $[Et_4N][$*fac*-$Mo(CO)_3[P(OMe)_3]_2SH]$, 116148-61-9; $[Et_4N][$*fac*-$Mo(CO)_3(PMe_3)_2SH]$, 116148-63-1; $[Et_4N][$*fac*-$Mo(CO)_3(dppe)SH]$, 116148-65-3; $[Et_4N][$*fac*-$Mo(CO)_3[P(OMe)_3]_2SPh]$, 116184-38-4; $[Et_4N][$*fac*-$Mo(CO)_3(PMe_3)_2SPh]$, 116148-67-5; $[Et_4N][$*fac*-$Mo(CO)_3(dppe)SPh]$, 116148-69-7; $[Et_4N][$*fac*-$W(CO)_3(PMe_3)_2SH]$, 116148-71-1; $[Et_4N][$*fac*-$W(CO)_3(dppe)SH]$, 116148-73-3; $[Et_4N][$*fac*-$W(CO)_3[P(OMe)_3]_2SPh]$, 116184-40-8; $[Et_4N][$*fac*-$W(CO)_3(PMe_3)_2SPh]$, 116184-42-0; $[Et_4N][$*fac*-$W(CO)_3(dppe)SPh]$, 116184-44-2; thiophenol, 108-98-5.

Supplementary Material Available: A thermal ellipsoid plot (50% probability) with numbering scheme for the Et_4N^+ ion (Figure 1S), a space-filling model of $W_2(CO)_8(\mu\text{-SPh})_2^{2-}$ (Figure 2S), a packing diagram of $[Et_4N]_2[W_2(CO)_8(\mu\text{-SPh})_2]$ (Figure 3S), crystallographic data (Table 1S), anisotropic displacement parameters (*U* values, Table 2S), and H atom coordinates and isotropic displacement parameters (Table 3S) (7 pages); calculated and observed structure factor amplitudes (Table 4S) (13 pages). Ordering information is given on any current masthead page.

---

(23) Kao, S. C.; Darensbourg, M. Y.; Schenk, W. *Organometallics* **1984**, *3*, 871.

(24) Darensbourg, D. J.; Kudaroski, R. *J. Am. Chem. Soc.* **1984**, *106*, 3672.

(25) Darensbourg, D. J.; Sanchez, K. M., unpublished observation.